

Europium substitution effects on structural, magnetic and magnetocaloric properties in $\text{La}_{0.5}\text{Ca}_{0.5}\text{MnO}_3$

A. Krichene^{1 a}, W. Boujelben^a and A. Cheikhrouhou^{a, b}

^a Laboratoire de Physique des Matériaux, Faculté des Sciences de Sfax, B. P. 1171, 3000 Sfax Tunisie

^b Institut NEEL, CNRS, B.P.166, 38042 Grenoble Cedex 9, France

Abstract. We have investigated structural, magnetic and magnetocaloric properties of polycrystalline samples $\text{La}_{0.5-x}\text{Eu}_x\text{Ca}_{0.5}\text{MnO}_3$ ($x=0$ and 0.1). Rietveld refinement of the X-ray diffraction patterns show that our samples are single phase and crystallize in the orthorhombic structure with Pnma space group. Magnetization measurements versus temperature at a magnetic applied field of 500 Oe indicate that $\text{La}_{0.4}\text{Eu}_{0.1}\text{Ca}_{0.5}\text{MnO}_3$ sample exhibits a paramagnetic to ferromagnetic transition with decreasing temperature. Magnetic measurements reveal strong magnetocaloric effect in the vicinity of the Curie temperature T_C . The parent compound shows a negative magnetic entropy change of $\Delta S_M = -1.13 \text{ J kg}^{-1} \text{ K}^{-1}$ at 220K and a positive magnetocaloric effects $\Delta S_M = 1 \text{ J kg}^{-1} \text{ K}^{-1}$ at 150K under a magnetic applied field of 2T. $\text{La}_{0.4}\text{Eu}_{0.1}\text{Ca}_{0.5}\text{MnO}_3$ exhibits a maximum value of magnetic entropy change $\Delta S_M = -1.15 \text{ J kg}^{-1} \text{ K}^{-1}$ at 130K under an applied field of 2T and a large relative cooling power RCP with a maximum value of 72 J/kg.

1 Introduction

The manganites with general formula $\text{Re}_{1-x}\text{Ae}_x\text{MnO}_3$, where Re is a rare earth (La, Pr, Nd...) and Ae is an alkaline earth (Ca, Sr, Ba...), have been deeply studied not only for the interesting phenomena that they have but also because of their technological applications in several domains (magnetic refrigeration, magnetic random access memory...) [1-5]. The $\text{La}_{1-x}\text{Ca}_x\text{MnO}_3$ has a rich phase diagram where the doping level x and the temperature determine the presence of paramagnetic, ferromagnetic, antiferromagnetism, orbital and charge ordering. The half doped perovskite manganites $\text{Ln}_{0.5}\text{A}_{0.5}\text{MnO}_3$ (Ln=rare earth, A= alkaline earth) attract great attention because they display rich physics including charge ordering (CO) and orbital ordering OO [6-12]. Investigations of charge ordering in the rare earth manganites have revealed extraordinary variety in the physical properties including their sensitivity to external factors such as the average size of the A-cation site, magnetic and electrical fields, hydrostatic pressure, as well as isotropic and chemical substitution [6,13,14]. $\text{La}_{0.5}\text{Ca}_{0.5}\text{MnO}_3$ is a typical system showing CO phenomena. It undergoes a paramagnetic

¹ e-mail : akramkri@hotmail.fr

to ferromagnetic transition at $T_c \approx 225\text{K}$, which followed by a transition to a charge ordered state with CE-Type antiferromagnetic structure at $T_{CO} = 150\text{K}$ during cooling sequence [15]. Recent studies indicate further that the kinetic hindrance to the first order transition has serious consequences on the coexisting phases [16, 17]. It is widely believed that the properties of manganese oxides are mainly determined by the $\text{Mn}^{3+}/\text{Mn}^{4+}$ ratio and the Mn-O-Mn bond angle, which affect the orbital overlapping between neighboring ions [6].

Our study has been carried out to investigate the effect of europium substitution on structural, magnetic and magnetocaloric properties in $\text{La}_{0.5}\text{Ca}_{0.5}\text{MnO}_3$.

2 Experimental techniques

Polycrystalline $\text{La}_{0.5-x}\text{Eu}_x\text{Ca}_{0.5}\text{MnO}_3$ ($x=0$ and 0.1) samples were prepared using the solid state reaction method at high temperatures. Stoichiometric quantities of La_2O_3 , Eu_2O_3 , CaCO_3 , and MnO_2 were intimately mixed in an agate mortar and then heated in air up to 800°C for 18 hours. The obtained powders were then pressed into pellets (of about 1mm thickness and 13mm diameter) and sintered at 1200°C in air for 60h with intermediate regrinding and repelling. Finally, these pellets were rapidly quenched to room temperature in air in order to freeze the structure at the annealed temperature. Phase purity, homogeneity and cell dimensions were determined by powder X-Ray diffraction at room temperature. Structural analysis was made using the standard Rietveld technique [18, 19]. The amount of Mn^{4+} ions has been quantitatively checked by chemical analysis. Magnetization measurements versus temperature in the range 10-300K and versus magnetic applied field up to 8T were carried out using a vibrating sample magnetometer. Magnetocaloric effects (MCE) were deduced from the magnetization measurements versus magnetic applied field up to 8T at several temperatures.

3 Results and discussion

3.1 Chemical analysis

As our samples have been synthesized in air, they are stoichiometric in oxygen [20]. For our both samples the $\text{Mn}^{4+}/\text{Mn}^{3+}$ amount equal to one theoretically, however the average ion radius of the A cation site $\langle r_A \rangle$ and the cationic disorder σ^2 changes.

The Mn^{4+} and Mn^{3+} contents have been checked by chemical analysis. We list in table 1 the chemical analysis results. The experimental analysis results show that the Mn^{4+} content for our samples are slightly smaller than the theoretical values. The ratio $\text{Mn}^{4+}/\text{Mn}^{3+}$ is equal to 0.95 for the parent compound and 0.99 for the europium substituted sample.

Table 1: Chemical analysis results for $\text{La}_{0.5}\text{Ca}_{0.5}\text{MnO}_3$ and $\text{La}_{0.4}\text{Eu}_{0.1}\text{Ca}_{0.5}\text{MnO}_3$ samples.

| Samples | experimental contents | |
|---|-----------------------|------------------|
| | Mn^{3+} | Mn^{4+} |
| $\text{La}_{0.5}\text{Ca}_{0.5}\text{MnO}_3$ | 51.31% | 48.69% |
| $\text{La}_{0.4}\text{Eu}_{0.1}\text{Ca}_{0.5}\text{MnO}_3$ | 50.15% | 49.85% |

3.2 Structural study

The X-ray diffraction study of all our samples was carried out at room temperature and the data were analyzed with the Rietveld refinement technique using Fullprof code. Figure 1 shows typical X ray powder diffraction patterns registered at room temperature for the parent compound $\text{La}_{0.5}\text{Ca}_{0.5}\text{MnO}_3$ and the substituted one $\text{La}_{0.4}\text{Eu}_{0.1}\text{Ca}_{0.5}\text{MnO}_3$. Both samples are single phase without any detectable impurity and crystallize in the orthorhombic system with Pnma space group.

We have summarized in table 2 the cell parameters, the unit cell volume, the average ionic radius in the A site $\langle r_A \rangle$ and the cationic disorder given by $\sigma^2 = \sum_i (y_i r_i^2 - \langle r_A \rangle^2)$ [21, 22] for our samples.

The europium substitution induces a decrease of the unit cell parameters and the unit cell volume comparing to the parent compound $\text{La}_{0.5}\text{Ca}_{0.5}\text{MnO}_3$. This decrease can be explained by the europium ionic radius (1.120\AA), which is smaller than that of lanthanum (1.216\AA). The influence of the A-site cation size can be explained by its ability to modify the Mn-Mn distance and the Mn-O-Mn angle and consequently the distortion of the ideal perovskite structure in which the Mn-O-Mn is equal to 180° . Europium ions with smaller ionic radius induce local distortions of the Mn-O-Mn angle in the system and consequently cause a random distribution of the magnetic exchange interactions. The internal stress caused by substituting of La^{3+} by Eu^{3+} may result in a larger rotation of the MnO_6 octahedra. Both samples present a ratio of $\frac{b}{\sqrt{2}} < a$, characteristic of a cooperative Jahn-teller deformation.

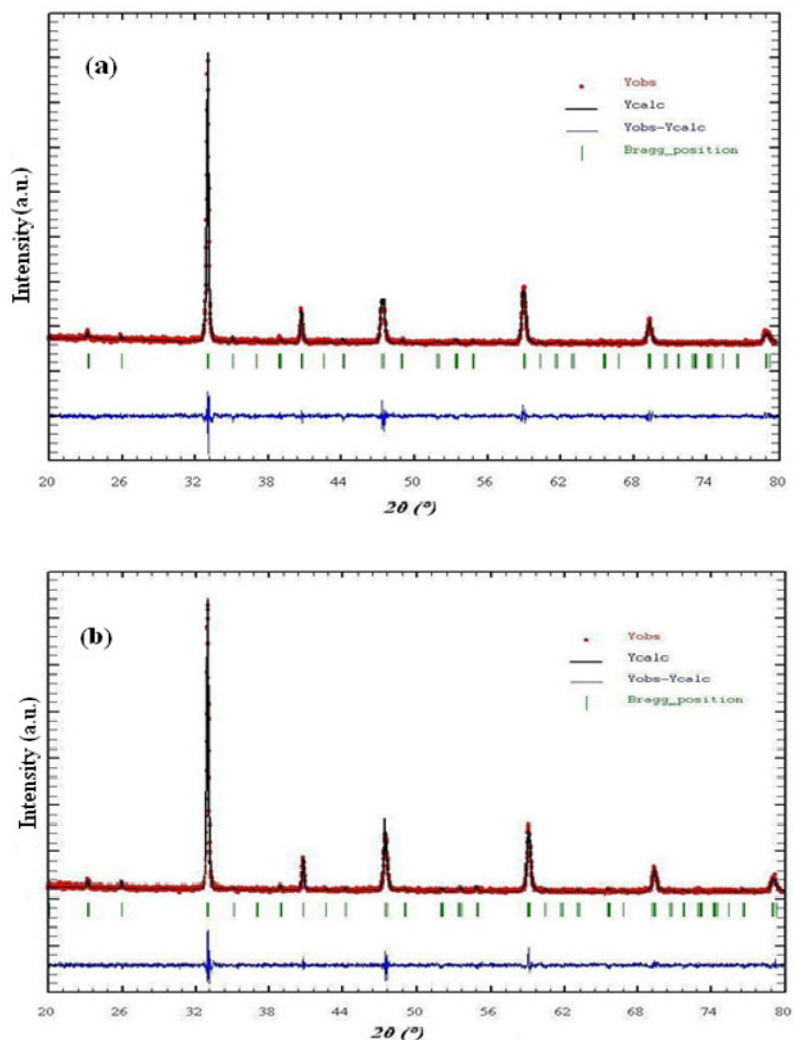


Fig.1. X-ray powder diffraction patterns and refinement for $\text{La}_{0.5}\text{Ca}_{0.5}\text{MnO}_3$ (a) and $\text{La}_{0.4}\text{Eu}_{0.1}\text{Ca}_{0.5}\text{MnO}_3$ (b) samples.

Table 2: Cell parameters, unit cell volume, $\langle r_A \rangle$ and σ^2 values for $\text{La}_{0.5-x}\text{Eu}_x\text{Ca}_{0.5}\text{MnO}_3$ ($x=0$ and 0.1) samples.

| Samples | a (Å) | b/ $\sqrt{2}$ (Å) | c (Å) | V (Å ³) | $\langle r_A \rangle$ (Å) | σ^2 (10 ⁻³ Å ²) |
|---|----------|-------------------|----------|---------------------|---------------------------|---|
| $\text{La}_{0.5}\text{Ca}_{0.5}\text{MnO}_3$ | 5.421(4) | 5.407(2) | 5.429(8) | 225.106(1) | 1.1980 | 0.3240 |
| $\text{La}_{0.4}\text{Eu}_{0.1}\text{Ca}_{0.5}\text{MnO}_3$ | 5.414(1) | 5.402(4) | 5.424(1) | 224.370(1) | 1.1884 | 0.8078 |

3.3 Magnetic study

The temperature dependence of magnetization and its derivate for the two compounds were shown in figure 2 and figure 3. For the parent sample $\text{La}_{0.5}\text{Ca}_{0.5}\text{MnO}_3$ we observe a PM to FM transition at the Curie temperature $T_C=220\text{K}$ followed by another transition from FM to FM canted state at $T_{C2}=150\text{K}$ with decreasing temperature. The second transition can be attributed to the coexistence of the ferromagnetic and antiferromagnetic clusters. Several studies have been performed on $\text{La}_{0.5}\text{Ca}_{0.5}\text{MnO}_3$ and have shown different magnetic behavior at low temperature. Tong et al. [23] show an AFM-CO state at low temperature. Walha et al. [24] show an antiferromagnetic behavior at low temperature with a very small ferromagnetic component. Schiffer et al. [25] show a PM to FM transition at the Curie temperature $T_C=220\text{K}$ followed by another transition from FM to AFM-CO state at $T_{CO}=180\text{K}$. The diversity of the magnetic state at low temperature confirms the critical composition of the $\text{La}_{0.5}\text{Ca}_{0.5}\text{MnO}_3$ and shows a destabilized state at low temperature as a function of the elaborating methods and also to the $\text{Mn}^{4+}/\text{Mn}^{3+}$ ratio. For our elaborated sample the charge ordering CO state is delocalized and we observe at low temperature a magnetization value equal to $10\text{Am}^2/\text{kg}$ at a magnetic applied field of 500 Oe. This effect can be explained by the experimental $\text{Mn}^{4+}/\text{Mn}^{3+}$ ratio non equal to 1.

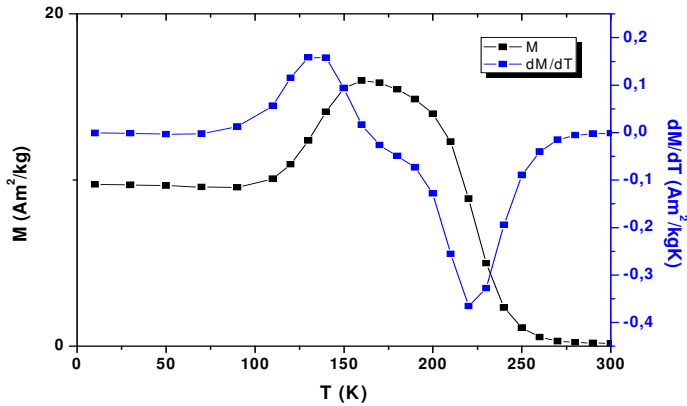


Fig. 2: Temperature dependence of magnetization and its derivate for $\text{La}_{0.5}\text{Ca}_{0.5}\text{MnO}_3$ sample at a magnetic applied field of 500 Oe.

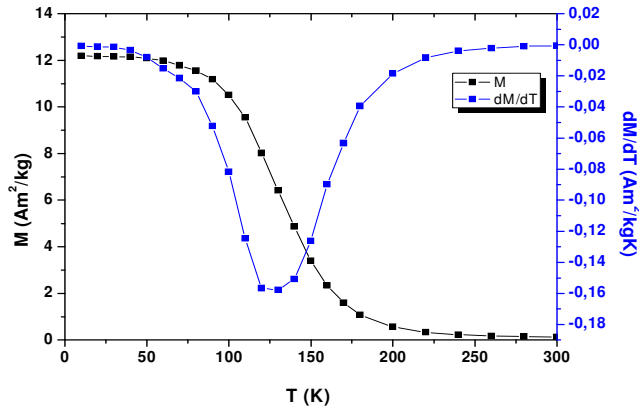


Fig.3: Temperature dependence of magnetization and its derivate for $\text{La}_{0.4}\text{Eu}_{0.1}\text{Ca}_{0.5}\text{MnO}_3$ simple at a magnetic applied field of 500 Oe

Figure 3 shows that the europium substitution destroys the second transition figuring at low temperature in the parent compound, enhances ferromagnetic state and that the Curie temperature decreases sharply to 130K. Our results are in agreement with those found in $\text{La}_{0.375}\text{Tb}_{0.125}\text{Ca}_{0.5}\text{MnO}_3$ [4], $\text{La}_{2/3-x}\text{Eu}_x\text{Ca}_{1/3-y}\text{Sr}_y\text{MnO}_3$ [26] and $\text{La}_{0.4}\text{Y}_{0.1}\text{Ca}_{0.5}\text{MnO}_3$ [27] systems.

The evolution of magnetization versus magnetic applied field at several temperatures for the both samples was reported in figure 4 and figure 5. The $M(H)$ curves for the both samples confirm the existence of different magnetic states as a function of temperature and confirm the results found with the $M(T)$ curves.

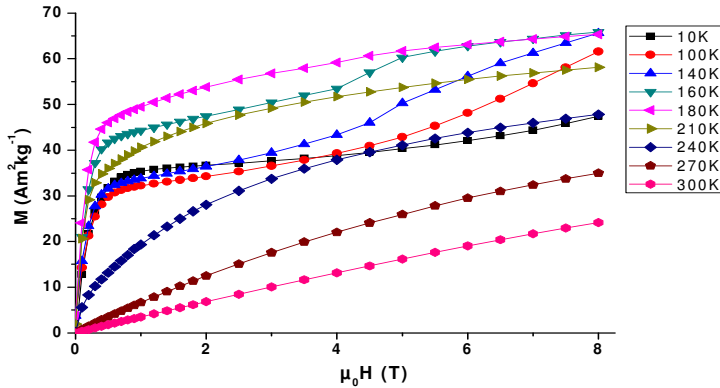


Fig.4: $M(H)$ curves at several temperatures for $\text{La}_{0.5}\text{Ca}_{0.5}\text{MnO}_3$ sample.

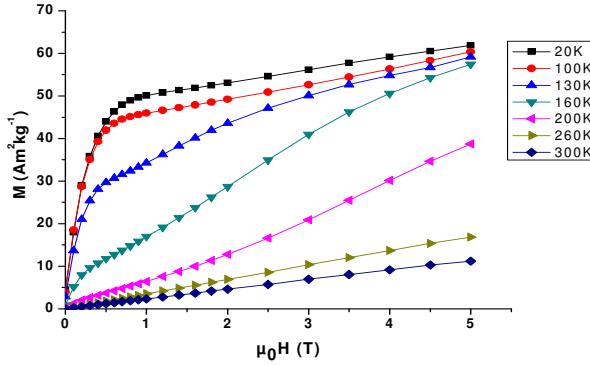


Fig. 5: $M(H)$ curves at several temperatures for $\text{La}_{0.4}\text{Eu}_{0.1}\text{Ca}_{0.5}\text{MnO}_3$ sample

3.4 Magnetocaloric study

The magnetic entropy change, ΔS , has been deduced from isothermal magnetization measurements. Based on Maxwell's relations, ΔS can be evaluated using the following equation:

$$\Delta S = \sum_i \frac{M_i - M_{i+1}}{T_{i+1} - T_i} \Delta H_i \quad (1)$$

where M_i and M_{i+1} are the experimental values of magnetization measured at temperatures T_i and T_{i+1} , respectively, under magnetic applied field H_i .

Temperature dependence of magnetic entropy change under a magnetic applied field of 2T for both samples $\text{La}_{0.5-x}\text{Eu}_x\text{Ca}_{0.5}\text{MnO}_3$ ($x=0$ and 0.1) was shown in Figure 6 and shows a broad peak around T_C with negative ΔS_M value and relatively narrow peak at T_{C2} with positive ΔS_M . The parent compound is characterized by two values of maximum entropy change, a positive maximum in the vicinity of the second transition at $T_{C2}=150\text{K}$ and a negative one in the vicinity of Curie temperature which is in agreement with previous works [25]. For europium substituted sample, only a negative maximum is seen in the vicinity of Curie temperature, the second maximum disappeared because of the destruction of the second transition existing at low temperature in $\text{La}_{0.5}\text{Ca}_{0.5}\text{MnO}_3$.

The ΔS_M is found to be -1.13Jkg/K and -1.15Jkg/K around T_C for respectively $\text{La}_{0.5}\text{Ca}_{0.5}\text{MnO}_3$ and $\text{La}_{0.4}\text{Eu}_{0.1}\text{Ca}_{0.5}\text{MnO}_3$. For $\text{La}_{0.5}\text{Ca}_{0.5}\text{MnO}_3$, ΔS_M is equal to 1Jkg/K at $T_{C2}=150\text{K}$.

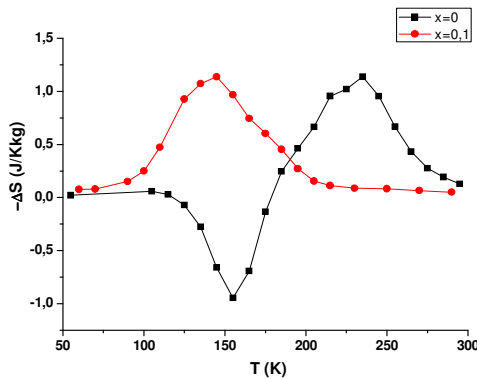


Fig. 6: Temperature dependence of magnetic entropy change for $\text{La}_{0.5}\text{Ca}_{0.5}\text{MnO}_3$ and $\text{La}_{0.4}\text{Eu}_{0.1}\text{Ca}_{0.5}\text{MnO}_3$ samples under a magnetic applied field of 2T

The relative cooling power (RCP) describing an amount of heat transported between temperatures corresponding to the half maximum width of ΔS peak, is evaluated as $RCP = -\Delta S_{\max} * \delta T_{FWHM}$, where δT_{FWHM} is the full-width at half-maximum of ΔS [28, 29].

In Table 3, we have summarized the values of T_C , $-\Delta S_{\max}$, and RCP for $La_{0.5-x}Eu_xCa_{0.5}MnO_3$ ($x=0$ and 0.1) samples under a magnetic applied field of 2T. Europium substitution enhances ferromagnetism state at low temperature but did not implicate a large magnetocaloric effect which can be explained by the cationic disorder induced by the europium substitution. A decrease of magnetocaloric effect was observed in the compounds $La_{2/3-x}Eu_xCa_{1/3-y}Sr_yMnO_3$ having the highest values of mismatch [26].

Table 3: T_C , $-\Delta S_{\max}$, and RCP values for $La_{0.5-x}Eu_xCa_{0.5}MnO_3$ ($x=0$ and 0.1) for an applied field of 2T.

| Samples | T_C (K) | $-\Delta S_{M \max}$ (Jkg ⁻¹ K ⁻¹) | RCP(J/kg) |
|---------------------------------|-----------|---|-----------|
| $La_{0.5}Ca_{0.5}MnO_3$ | 220 | 1.13 | 68 |
| $La_{0.4}Eu_{0.1}Ca_{0.5}MnO_3$ | 130 | 1.15 | 72 |

4 Conclusions

We have investigated structural, magnetic and magnetocaloric properties of $La_{0.5-x}Eu_xCa_{0.5}MnO_3$ samples ($x=0$ and 0.1). Structural analysis shows that our samples crystallize in the orthorhombic structure with Pnma space group. The europium substitution induces a decrease of the unit cell volume which can be explained by the decrease of the average ionic radius in A site $\langle r_A \rangle$.

Magnetic measurements show that the europium substitution enhances ferromagnetism and destroys the second transition observed in the parent compound at low temperatures. The $La_{0.4}Eu_{0.1}Ca_{0.5}MnO_3$ sample has an absolute value of magnetic entropy change which is near to $La_{0.5}Ca_{0.5}MnO_3$ one.

References

1. H. Kuwahara, Y. Tomioka, A. Asamitsu, Y. Moritomo, Y. Tokura, Science, **270** 961 (1995)
2. R. Mahendiran, M.R. Ibarra, A. Maignan, C. Martin, B. Raveau, A. Hernando, Solid State Comm. **111** 525 (1999)
3. A. Banerjee, K. Kumar, P. Chaddah, J. Phys.: Condens. Matter, **20** 255245 (2008)
4. R. R. Doshi, P. S. Solanki, U. Khachar, D. G. Kuberkar, P.S.R. Krishna, A. Banerjee, P. Chaddah, Physica B **406** 4031 (2011)
5. G. J. Liu, J.R. Sun, B.G. Shen, Solid State Comm. **149** 722 (2009)
6. J. Jin, T. H Tidfel, M. Mc Cormack, R. A. Fastnacht, R. Ramesh, L. H. Chen, Science, **264** 413 (1994)
7. C. N. Rao, A. Arulaj, A.K. Cheetman, B. Raveau, J. Phys.:Condens. Matter, **12** R83 (2000)
8. J. M. D. Coey, M. Viret, S. Von Molnar, Adv. Phys. **48** 167 (1999)
9. R. Ang, Y.P. Sun, X.B. Zhu, W.H. Song, Solid State Comm. **138** 505 (2006)
10. W. W. Gao, J. R. Sun, X. Y. Lu, D. S. Shang, J. Wang, F. X. Hu, B. G. Shen, J. Appl. Phys.: **109** 07C729 (2011)
11. I. Dhiman, A. Das, P.K. Mishra, N.P. Lalla, A. Kumar, J. Magn. Magn. Mater. **323** 748 (2011)
12. C. Krishnamoorthi, S.K. Barik, Z. Siu, R. Mahendiran, Solid State Comm. **150** 1670 (2010)
13. Y. Tomioka, A. Asamitsu, H.Kuwara, Y. Moritomo, Y. Tokura, Phys. Rev. B **53** R1689 (1996)
14. Y. Moritomo, H. Kuwahara, Y. Tomioka, Y. Tokura, Phys. Rev. B **55** 7549 (1997)
15. P. Levy, F. Parisi, G. Polla, D. Vega, G. Leyva, H. Lanza, R. S.Freitas, L. Ghivelder, Phys. Rev. B **62** 6437 (2000)
16. A. Chaddah, K. Kumar, A. Banerjee, Phys. Rev. B **77** 100402 (R) (2008)
17. A. Banerjee, K. Kumar, P. Chaddah, J. Phys.: Condens. Matter. **20** 255245 (2008)
18. H. M. Rietveld, J. App. Cryst. **2** 65 (1969)

- 19 T. Roisnel, J. Rodriguez-Carvajal, Computer program FULLPROF, LLB-LCSIM. May 2003
- 20 J. H. Kuo, H.U. Anderson, D.M. Sparlin, J. Solid State Chem. **83** 52 (1989)
- 21 L. M. Rodriguez-Martinez, J.P. Attfield, Phys. Rev. B **54** R15622 (1996)
- 22 L. M. Rodriguez-Martinez, J.P. Attfield, Phys. Rev. B **58** 2426 (1998)
- 23 W. Tong, T. Tang, X. Liu, Y. Zhang, Phys. Rev. B **68** 134435 (2003)
- 24 I. Walha, H. Ehrenberg, H. Fuess, A. Cheikhrouhou, J. Alloys compd. **433** 63 (2007)
- 25 P. E. Schiffer, A. P. Ramirez, W. Bao, S. W. Cheong, Phys. Rev. Letter, **75** 3336
- 26 Q. Xie, B. Lv, P. Wang, P. Song, X. Wu, Mater. Chem. Phys. **114** (2009) 636 (1995)
- 27 P. D. Babu, A. Das, S.K. Paranjpe, Solid State Comm. **118** 91 (2001)
- 28 V. K. Pecharsky, K.A. Gschneidner, Annu.Rev. Mater. Sci. **30** (2000) 387
- 29 V. K. Pecharsky, K.A. Gschneidner, A.O. Tsokol, Rep. Prog. Phys. **68** 1479 (2005)